Resonant Hydrophones Based on Coated Fiber Bragg Gratings

Massimo Moccia, Marco Consales, Agostino Iadicicco, Marco Pisco, Antonello Cutolo, Vincenzo Galdi, *Senior Member, IEEE*, and Andrea Cusano

***Abstract*—In this paper, we report on recent experimental results obtained with fiber-Bragg-grating (FBG) hydrophones for underwater acoustic detection. The optical hydrophones under investigation consist of FBGs coated with ring-shaped polymers of different size and mechanical properties. The coating materials were selected and designed in order to provide mechanical amplification, via judicious choice of their acousto-mechanical properties and by exploiting selected resonances occurring in different frequency ranges. Our underwater acoustic measurements, carried out within the range 4–35 kHz, reveal the resonant behavior of these optical hydrophones, as well as its dependence on the coating size and type of material. These experimental data are also in good agreement with our previously published numerical results. By comparison with bare (i.e., uncoated) FBGs, responsivity enhancements of up to three orders of magnitude were found, demonstrating the effectiveness of polymeric coatings in tailoring the acoustic response of FBG-based hydrophones.**

***Index Terms*—Fiber Bragg gratings (FBGs), fiber-optic sensors, in-fiber hydrophones.**

I. Introduction

SINCE the first demonstration in the 1970s [1], [2], fiber-optic acoustic sensors have been extensively studied for several application areas, such as structural health, marine monitoring, as well as military and medical detections [3], [4]. By comparison with conventional piezoelectric (PZT) hydrophones, fiber-optic sensors have the advantages of providing high sensitivity, large dynamic range, convenience for multiplexing, flexibility of design, immunity to electromagnetic interference, absence of electrical parts, especially important for underwater applications [3], [4].

Recent papers by Wild and Hinckley [4], Culshaw *et al.* [5], Thursby *et al.* [6], and Kirkendall and Dandridge [7] provide comprehensive reviews of the state of the art of optical fiber acoustic and ultrasonic sensing, summarizing the vast majority of sensing methods and techniques currently available in the literature. Although fiber-optic hydrophones based on various principles of operation have been demonstrated [4], a promising hydrophone scheme relies on the use of the well-known fiber Bragg gratings (FBGs) [8]–[11]. Besides the aforementioned advantages, common to all fiber-optic sensors, FBGs allow easy configurations, can work in reflectivity mode, and, most importantly, offer excellent multiplexing capabilities.

Acoustic monitoring for underwater applications is also an important area of interest where FBG-based hydrophones have gained large popularity [12]–[19]. Since the first demonstration by Hill and Nash[13], several studies based on active FBG acoustic sensor configurations have been carried out [12], [14], [20]–[24]. For instance, Goodman *et al.* [20] proposed a distributed feedback (DFB) fiber laser hydrophone with a frequency responsivity of 108 dB re Hz/Pa. Zhang *et al.* [21] proposed a DFB fiber laser hydrophone based on double diaphragms, which exhibited a maximum responsivity of 7 nm/MPa, with a minimum detectable acoustic signal of 140 $\mu\mathrm{Pa}\sqrt{\mathrm{Hz}}$ at 1 kHz. Ma *et al.* [22] proposed a DFB fiber laser hydrophone with a novel mounting structure, which exhibited a responsivity up to 102.77 dB reHz/Pa and a fluctuation of less than 1.5 dB within 2.5 kHz. Even though DFB fiber laser hydrophones provide unique characteristics combined with good multiplexing capability, they require sophisticated configurations involving active doped fibers, pump laser, etc. [25].

Alternative configurations, which provide significant benefits in the sensor use and interrogation units, involve passive FBG schemes. Takahashi *et al.* [8], [15] proposed the use of FBGs as underwater acoustic sensors by monitoring the light intensity transmitted through the grating. The operating principle relies on the shift in the reflected/transmitted spectrum of the grating caused by the sound pressure. Improvements in the hydrophone response were obtained with temperature compensation [16], [17], by using feedback control and multipoint sensing configurations [18], [19]. Unfortunately, in the case of uncoated FBGs, the mechanical deformation of the fiber due to the incident pressure is limited by the high Young's modulus (72 GPa [26]), leading to a poor responsivity at very low pressure levels.

An effective strategy to overcome this limitation was suggested by Hocker [27]–[29], by recognizing that low-elastic-modulus ring-shaped coatings may yield significant pressure responsivities. Starting from this work, FBGs coated with materials characterized by Young's modulus lower than that of the fiber glass were proposed as promising hydrostatic pressure sensors [26], [30]. Although the theoretical/numerical analysis carried out by Hocker [27]–[29] was limited to the hydrostatic case and cannot rigorously be extended to the acoustic case, experimental evidence of acoustic responsivity optimization in the case of coated FBGs has been recently demonstrated by the

Manuscript received October 14, 2011; revised February 29, 2012, April 24, 2012; accepted April 28, 2012. Date of publication May 18, 2012; date of current version July 04, 2012.

M. Moccia, M. Consales, M. Pisco, A. Cutolo, and A. Cusano are with the Optoelectronic Division, Department of Engineering, University of Sannio, I-82100 Benevento, Italy (e-mail: massimo.moccia@unisannio.it; consales@unisannio.it; pisco@unisannio.it; cutolo@unisannio.it; a.cusano@unisannio.it).

A. Iadicicco is with the Department for Technology, Parthenope University of Naples, I-80143 Napoli, Italy (e-mail: iadicicco@uniparthenope.it).

V. Galdi is with the Waves Group, Department of Engineering, University of Sannio, I-82100 Benevento, Italy (e-mail: vgaldi@unisannio.it).

Color versions of one or more of the figures in this paper are available online at http://ieeexplore.ieee.org.

Digital Object Identifier 10.1109/JLT.2012.2200233

authors in [31] and [32]. In order to clearly understand to what extent the static analysis in [27]–[29] could be extended also to acoustic scenarios, we recently carried out a rigorous numerical study of FBGs coated with cylindrically shaped polymeric materials, via numerical (finite-element) solution of the complex opto-acousto-mechanical problem in the acoustic wave range (up to 30 kHz) [33], [34]. We found that, similar to the static pressure case, also in the acoustic range a polymeric coating is actually able to enhance the sensor responsivity. However, unlike the static case, free vibration modes of the composite structure may be excited at certain acoustic wavelengths, depending on the coating properties (e.g., Young's modulus, acoustic impedance, Poisson ratio, and acoustic damping). As a result, the acoustic response of coated FBG hydrophones exhibits a resonant behavior at the frequencies corresponding to these longitudinal symmetric vibration modes [34]. The main outcome of this analysis is the possibility to tailor the acoustic performances of coated FBGs via judicious selection of the ring-shaped coating, which opens up new venues for the development of fiber-optic hydrophones [34].

Against the aforementioned background, this work reports for the first time (to the best of our knowledge) a systematic and accurate experimental characterization of coated FBG hydrophones. This experimental study also serves as a validation of our previously published numerical results [34]. In particular, we designed a set of FBG hydrophones with ring-shaped coatings characterized by different size and mechanical properties, in order to elucidate their impact on the acoustic response of the final device. These hydrophones were fabricated and experimentally characterized within the frequency range 4–35 kHz by means of a suitably equipped tank [35]. Outcomes from a preliminary offshore demonstration of a ring-shaped coated FBG hydrophone are also reported and discussed.

II. Sensor Design

Based on our previous numerical results [34], we designed a suitable set of FBG hydrophones, taking into account three main objectives:

1) to experimentally demonstrate the resonant behavior in the responsivity (insofar observed only numerically);
2) to analyze the influence of the cylindrical coating features on such resonant behavior;
3) to fabricate several hydrophones characterized by different spectral responses and, more specifically, with resonances at frequencies lower and higher than 15 kHz.

Following [33] and [34], the polymeric coatings were properly selected to provide resonant features in the two selected ranges. In particular, coatings based on materials with low Young's modulus were designed so as to yield resonances occurring in the low-frequency range, whereas materials with high Young's modulus were exploited in the high-frequency range [34].

Two different coating materials were selected, characterized by relatively "low" and "high" Young's modulus: Damival E 13650 and Araldite DBF. The former is a polyurethane resin, commonly used to overcoat piezoceramic acoustic transducers without degrading their performance, which exhibits Young's modulus on the order of few hundred MPa, and acoustic impedance matching that of water. The latter is a low-viscosity epoxy resin containing a plasticizer, typically used as strong adhesive, and characterized by Young's modulus of 2.9 GPa [36]. These two materials are also characterized by significantly different loss factors, as discussed in detail hereafter [37]–[42].

TABLE I
Properties of the Coating Materials Used in our Numerical Analysis

Elastic Properties	Damival® E 13650	Araldite® DBF
Young's modulus (E)	200MPa	2.9GPa
Poisson's ratio (ν)	0.4	0.345
Loss factor (η)	0.1	$2\ 10^{-2}$
Density (ρ')	$1180 kg/m^3$	$1100 kg/m^3$

Overall, we analyzed numerically [34] and experimentally three sensors with the following characteristics:

1) Damival sensor, with coating diameter and length of 5 and 40 mm, respectively;
2) Araldite sensor, with coating diameter and length of 5 and 38 mm, respectively
3) Damival sensor, with coating diameter and length of 10 and 40 mm, respectively.

In our numerical simulations, we assumed for both materials the same mechanical properties considered in [34], and summarized in Table I.

In what follows, the frequency responses of the FBG hydrophones under investigation are shown in terms of the "responsivity gain" (RG) with respect to the uncoated FBG (also referred to as "sensitivity gain" [33], [34])

$$\mathrm{RG} = 20 \log_{10} \left(\left| \frac{R}{R_{\mathrm{BARE}}} \right| \right) \tag{1}$$

where $R_{\mathrm{BARE}} = -2.76 \times 10^{-6}\ \mathrm{MPa}^{-1}$ is the responsivity (also referred to as "sensitivity" [33], [34]) of the uncoated FBG [26], [29], and R is the sensor responsivity in terms of normalized wavelength shift

$$R = \frac{\Delta\lambda}{\lambda_0 P_0} \tag{2}$$

with $\Delta\lambda/\lambda_0$ denoting the relative Bragg wavelength shift, and P_0 is the amplitude of the sound pressure.

In Fig. 1(a), the simulated RG spectra of Damival and Araldite hydrophones (5 mm diameter) are shown. These numerical results confirm the resonant behavior for the two FBG hydrophones, with the spectral responses characterized by one or more resonant peaks. It is also possible to notice the presence of narrow-band dips, close to the resonant frequencies, which can be attributed to the damping factor [34]. In particular, the presence of the dips is more relevant for resonances occurring at high frequencies.

Moreover, it is important to highlight that, as expected, the two spectra reported in Fig. 1(a) exhibit strong differences, mainly attributable to the different mechanical parameters (and, in particular, to the Young's modulus) of the involved coatings. More specifically, the Damival sensor exhibits a high background RG ($\sim$47 dB at low frequencies) in agreement with the static model [27]–[29], whereas around the first resonance (5.4 kHz), the RG reaches the value of 65 dB. Moreover, the background RG slightly decreases with the acoustic frequency with a consequence desensitization at high

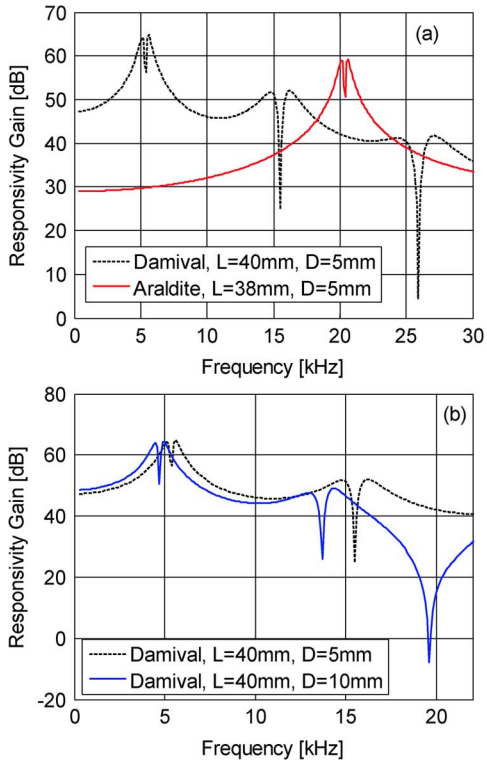

Fig. 1. Simulated RG spectra of Damival- and Araldite-based sensors.

frequencies (RG $<$ 42 dB above 20 kHz). Conversely, the Araldite hydrophone exhibits a static pressure gain of 39 dB, significantly lower than the Damival counterpart (47 dB), while the first resonance occurs around 21 kHz. Here, the maximum RG is $\sim$62 dB. Although a decrease of the background RG with the acoustic frequency is expected also in this case, this is not observable within the range considered.

In light of the aforementioned results, it clearly appears that Araldite-based sensors are much better suited to operate in the high-frequency range (15–30 kHz) than the Damival-based ones, which instead perform better within the range 0–20 kHz.

In Fig. 1(b), the simulated spectra of the two Damival sensors (5 and 10 mm diameter, respectively) are compared. As expected, increasing the diameter from 5 to 10 mm yields a downshift of all resonances, with the first resonance moving from 5.4 to 4.7 kHz. Moreover, it also yields a slight enhancement ($\sim$1.5 dB) of the background responsivity at low frequency (0–3 kHz). This is also in agreement with the numerical analysis in [28], which predicted a saturation effect occurring for diameter values above 5 mm, consistently with the static model [27]–[29].

Finally, it can be observed that the cutoff frequency of the "low-pass" behavior exhibited by the background responsivity decreases with the diameter. This is attributable to the acoustic diffraction, whose effects become relevant at lower frequencies when thicker coatings are considered.

III. Sensor Fabrication and Characterization Tools

The fabrication of the designed FBG hydrophones was carried out by means of a set of appropriate holders. In particular, for Damival-based sensors, a modular holder was designed so as to obtain a cylindrical coating on the fiber grating with desired size (in terms of sensor diameter and length). Moreover, in order to reduce mechanical stresses on the lead-in and lead-out fiber cables, the holder was designed so as to leave two conical regions (of the same material, and $\sim$10 mm long) on both ends of the cylindrical region. Such modular holder enabled for the realization of Damival sensors with diameter of 5 and 10 mm (henceforth, simply referred to as D-5 and D-10, respectively), while the length (selectable with steps of 10 mm) was fixed at 30 mm for both sensors. Taking into account the conical regions at the coating terminations, an effective length of 40 mm was estimated and considered in the numerical simulations. D-5 and D-10 sensors were fabricated using commercial UV-written fiber gratings (provided by O/E Land Inc., Lasalle, QC, Canada), with Bragg wavelengths of 1532.34 and 1555.75 nm, respectively, and bandwidths of 605 and 660 pm, respectively. A picture of sensor D-5 is shown in Fig. 2(a).

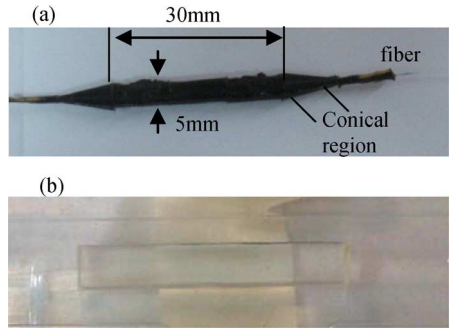

Fig. 2. Pictures of FBG hydrophones (a) D-5 and (b) A-5.

Conversely, in view of its low viscosity and high adhesive characteristics, a different configuration was implemented for the Araldite-based sensor. In this case, the holder (with diameter and length of 5.0 and 38 mm, respectively) is nonmodular in order to avoid the resin insertion between the modules, and there are no conical regions at the ends. Also this sensor (henceforth, A-5) was realized using a commercial UV-written fiber grating, with Bragg wavelength and bandwidth of 1547.80 and 410 pm, respectively. A picture of sensor A-5 is shown in Fig. 2(b).

Field trials were carried out in a state-of-the-art tank at the Whitehead Alenia Sistemi Subacquei Laboratory (Naples, Italy), with size 11 m $\times$ 5 m and depth 7 m, schematically depicted in Fig. 3. The tank is equipped with two PZT acoustic sources that can radiate sound pressure modulated pulses with Gaussian envelope and center frequency of 8 and 28 kHz. The combination of the two acoustic sources enables for a complete sensor characterization within the range 4–35 kHz. The tank is also equipped with a PZT reference hydrophone (Type 8104, from Bruel & Kjaer) which exhibits an almost constant responsivity of -209 ± 0.9 dB re(V/μPa) in the investigated frequency range. The acoustic sources and hydrophones (FBG and PZT) were positioned 3 m below the water level, while the distance from the PZT sources was $\sim$2 m for the reference hydrophone and $\sim$3 m for the FBG hydrophone. The FBG hydrophones were maintained vertically by a few gram weight and, consequently, the sound pressure was perpendicular to the fiber longitudinal axis.

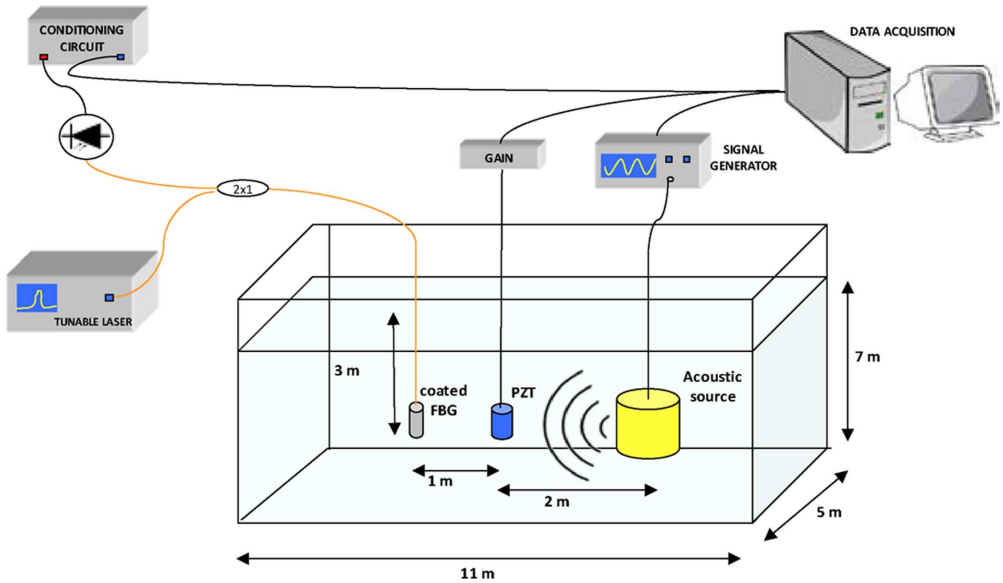

Fig. 3. Schematic of the instrumented tank and characterization setup.

In order to detect the Bragg wavelength shift induced by the sound pressure impinging on the coated devices, an edge-triggered narrow-band interrogation was used (see [31] and [32] for more details). To this aim, a tunable laser was utilized to lock the operating wavelength on the linear edge of the grating response. In this configuration, since the FBG spectrum shifts without changing its shape [15], [16], [31], [32], [35], the reflection variation at the laser wavelength is expected to be proportional to the applied pressure. The optoelectronic setup thus consisted of a tunable laser (Yokogawa AQ2200-136), a 2×1 directional coupler (capable of splitting the transmitted and reflected signals), and a photodiode (providing an electrical output proportional to the optical power reflected by the grating edge at the laser wavelength).

Finally, the electronic signal was suitably processed via a high-speed conditioning circuit that exhibits a tunable gain, adequate bandwidth, and low power consumption. Such circuit involves a modular multistadium ac-coupled trans-impedance amplifier which converts the photodiode current into a voltage. In particular, the circuit uses four amplifier modules operating in different acoustic frequency (3 dB) bandwidth such as 2–10, 10–15, 15–20, and 20–35 kHz. Furthermore, the circuit allows to tune the electronic gain up to 62 dB, in order to obtain a suitable electric signal amplitude. The amplified electronic signal is then sent to the data acquisition station, and stored at 400 k samples/s [35].

In order to characterize the performance of the optical sensors, as well as their dependence on the coating properties and size, the Bragg wavelength shift $\Delta\lambda$ induced by the acoustic pulse was retrieved via a simple normalization procedure

$$\Delta\lambda(t) = \frac{1}{\alpha}\,\frac{V_{\mathrm{ac}}(t)}{G_{\mathrm{ac}}} \tag{3}$$

with $V_{\mathrm{ac}}(t)$ denoting the ac output voltage at the final stadium of the conditioning circuit, G_{ac} is the amplification of the conditioning circuit, and α is the conversion factor strictly dependent on the slope of the linear edge of the FBG reflected spectrum evaluated at the working point. Via dedicated experimental tests, α values of 99.364, 89.108, and 122.227 mV/pm were estimated for the D-5, D-10, and A-5 sensors, respectively.

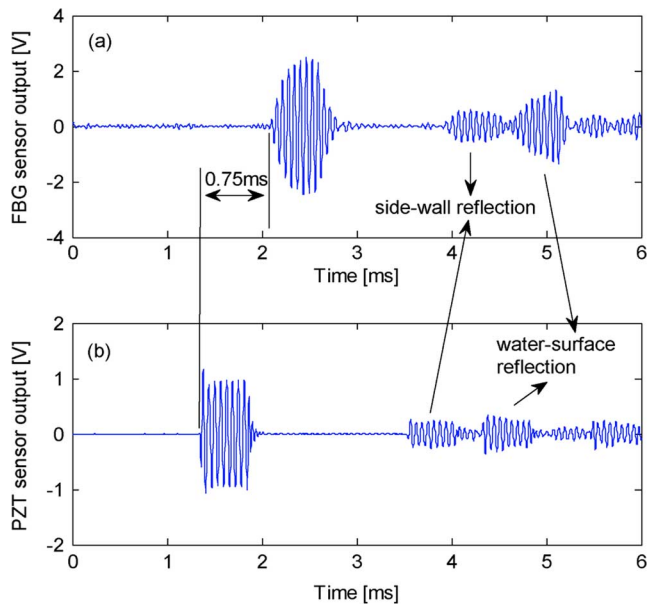

Fig. 4. Typical time responses of (a) FBG sensor D-5 and (b) PZT reference hydrophone to a 16 kHz acoustic pressure pulse of duration 0.5 ms and amplitude $\sim$32 Pa.

IV. Experimental Results

We now move on to illustrate the experimental results obtained using the FBG hydrophones D-5, D-10, and A-5, with the aim of validating the numerical predictions in Section II. In particular, attention was focused on the responses to an acoustic pressure pulse with frequency varying within the range 4–35 kHz, and amplitude ranging between 2 and 154 Pa.

A. Time Response

Fig. 4(a) shows a typical time response of sensor D-5 to a 16 kHz acoustic pressure pulse, with duration 0.5 ms and amplitude $\sim$32 Pa, as retrieved at the output stage of the conditioning

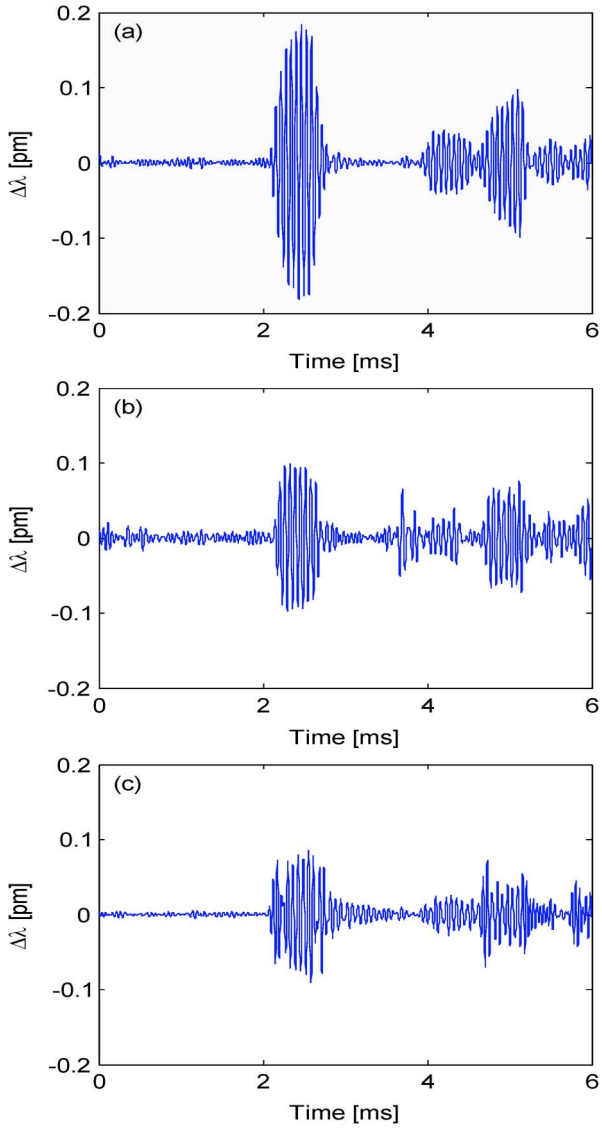

Fig. 5. Typical time responses in terms of wavelengths shift of FBG sensors (a) D-5, (b) D-10, and (c) A-5 to a 16 kHz acoustic pressure pulse with duration 0.5 ms.

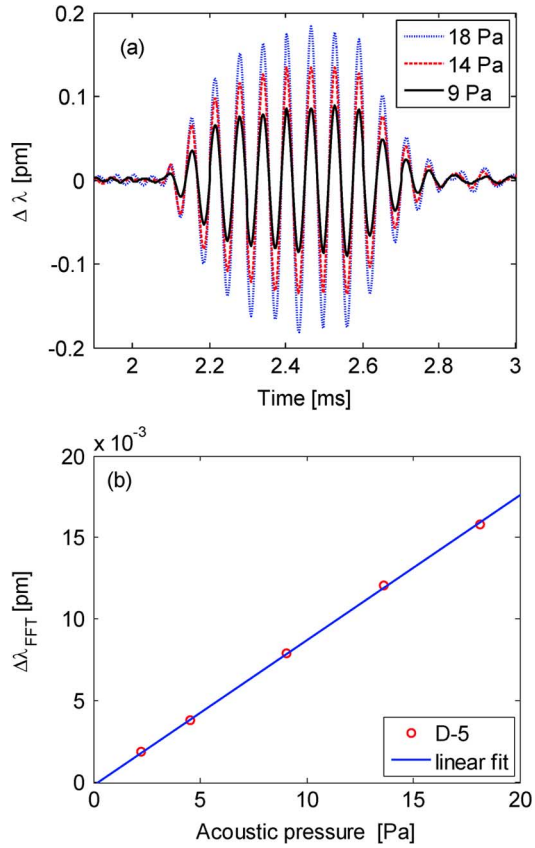

Fig. 6. Linearity analysis of sensor D-5. (a) Typical time responses to an acoustic pressure pulse at 16 kHz with different amplitudes. (b) Wavelength change (at 16 kHz) as a function of the acoustic pressure amplitude.

circuit. For comparison, the response of the PZT reference hydrophone is also shown in Fig. 4(b). As evident, both devices exhibit a quasi-sinusoidal response as the acoustic wave impinges on the sensor surface. While both signals are triggered at the sound excitation time, the optical signal is delayed with respect to the electric counterpart. Such delay ($\sim$0.75 ms) is due to the longer distance (1 m) at which the FBG hydrophone is located from the acoustic sources (by comparison with the PZT device), according to the schematic in Fig. 3.

The different position of the two hydrophones is also the cause of the phase difference occurring between their responses, and makes the optical fiber device to experience a lower pressure amplitude (32 Pa) than the PZT one (48 Pa), due to energy spreading losses [43].

The results in Fig. 4 clearly evidence the capability of both devices to detect not only the generated direct wave emitted by the acoustic source (i.e., the one that directly reaches the sensors without undergoing reflections), but also the weak contributions due to spurious reflections from the tank sidewalls and water surface.

In order to better characterize the sensors performance, we also took into account the time evolution of the Bragg wavelength shift [cf., (3)]. The Bragg wavelength shifts for sensors D-5, D-10, and A-5 are shown in Fig. 5(a)–(c), respectively.

In connection with the sensor linearity, the voltage applied to the electro-acoustic transducers was properly tuned in order to generate a series of acoustic-pressure pulses with increasing intensities (between 2 and 154 Pa). The linearity analysis was carried out for all frequencies within the range 4–35 kHz. The pressure levels, however, were not the same in the whole range due to the resonant behavior of the acoustic sources used in the experiments.

Fig. 6(a) shows the Bragg wavelength variation $\Delta\lambda$ pertaining to sensor D-5 for acoustic pulses of increasing amplitude at 16 kHz and duration 0.5 ms, which confirms the dependence of the optical response amplitude on the acoustic pressure amplitude. Fig. 6(b) shows the FBG wavelength shift $\Delta\lambda_{FFT}$, i.e., the peak value in the fast-Fourier-transform (FFT) spectrum of the time response, as a function of the amplitude of the applied sound pressure at 16 kHz for sensor D-5, together with its linear regression. From the linear fitting (exhibiting a coefficient of determination R^2 of 0.99955), the linear behavior of the sensor can be clearly observed, with the slope of the fitting curve estimated to be about 8.86×10^{-4} pm/Pa (with a standard error of 1.08×10^{-5} pm/Pa).

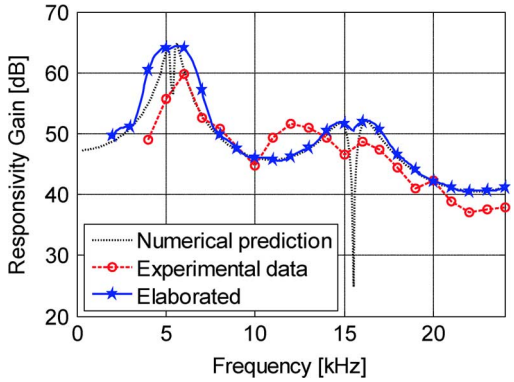

Fig. 7. Experimental and numerical RG of the optical sensors D-5 as a function of acoustic frequency.

Finally, it is worth highlighting that similar linear behaviors were observed for all fabricated FBG hydrophones, and that such behaviors were not affected by changes in the sound pressure frequency.

B. Frequency Domain Analysis

Next, we illustrate the spectral characterization of the fabricated hydrophones.

To this aim, the optical signal was measured for different acoustic pressure pulses with increasing frequency within the range 4–35 kHz (with 1 kHz step). In particular, the frequency response is shown here in terms of RG as expressed in (1), considering $\Delta\lambda_{\mathrm{FFT}}$ as the FBG wavelength shift (similar to the linearity analysis), λ_0 is the sensor Bragg wavelength (given in Section III), and P_0 is retrieved by means of the reference PZT hydrophone.

In Fig. 7, the spectral response of sensor D-5 is compared with the results from the previously described numerical analysis. A reasonably good agreement between experimental and numerical results can be observed. The spectral response is characterized by several peaks superimposed on a slightly decreasing (for increasing acoustic frequencies) background. A notable difference is the presence of narrow-band peaks in the numerical response, but not in the experimental one. As anticipated in Section II, such narrow dips in the RG spectra are attributable to the damping factor (see [34] for more details). In the experimental spectrum, these narrow spectral features cannot be observed because of the inherent limitations in the spectral resolution due to the finite time duration of a single acoustic tone (0.5 ms). On the other hand, the use of a finite-duration acoustic tone in the experimental measurements is mandatory, in order to avoid the superposition of the direct wave with the reflected ones from the tank wall and water surface. On the basis of these considerations, in order to better compare numerical and experimental data, the numerical RG was also computed by taking into account the finite duration (0.5 ms) of the input sine-wave pulses in the experimental characterization.

The obtained results (referred to as "elaborated") are also shown in Fig. 7, clearly revealing that the finite duration of the sine-wave pulses smoothes out the sharp spectral features, thereby strongly deemphasizing the narrow dips. As a result, the elaborated numerical spectrum (accounting for finite time duration) is in much better agreement with the experimental

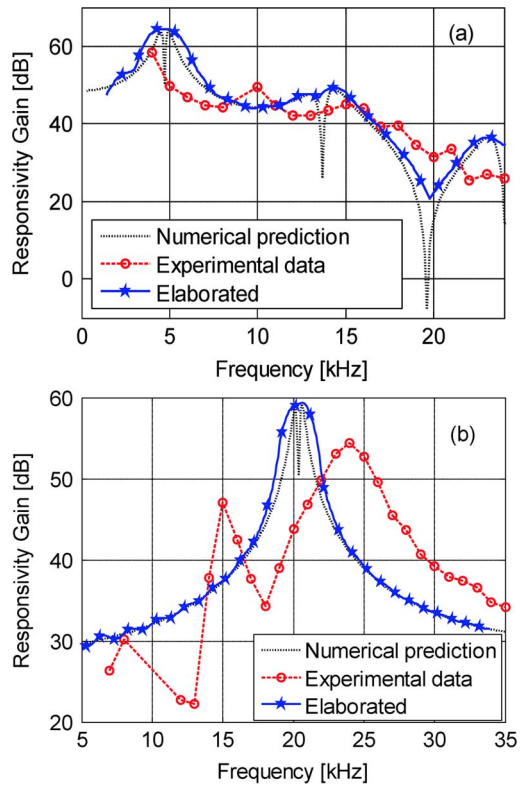

Fig. 8. Experimental and numerical RG spectra of the optical sensors (a) D-10 and (b) A-5, as a function of acoustic frequency.

one. The remaining slight disagreements can be attributed to second-order effects (physical imperfections, acoustically induced particle fluid motion, etc.), which are not taken into account in the simulations, but do not affect the basic transduction mechanism.

For a more quantitative assessment of the responsivity improvements endowed by the coated (versus uncoated) FBG sensors, with special emphasis on those induced by resonant effects, we point out that an amplification of three orders of magnitude was found at the first resonance (around 6 kHz, with RG ~ 61.4 dB), and of approximately two orders of magnitude for the background value. It is also worth noting that, as predicted by our numerical analysis, the background responsivity of the optical hydrophone exhibits a "low-pass" behavior attributable to acoustic diffraction.

Similar results have been obtained for sensor D-10 and A-5, whose numerical and experimental spectral responses are shown in Fig. 8(a) and (b), respectively. Also in these cases, elaborated numerical curves are added for a more accurate comparison.

A quite good agreement between experimental and numerical results can still be observed for these two sensors. The disagreements, mainly visible in the resonance frequencies and especially of sensor A-5 (centered at ~ 21 and 24 kHz in the numerical and experimental curves, respectively), can be attributed to slight physical imperfections or geometrical size inaccuracies in the fabricated device, although a thorough understanding of this aspect requires further study that is currently under way.

Nevertheless, it is worth emphasizing that, as predicted by our numerical simulations, the first resonance of the Araldite-

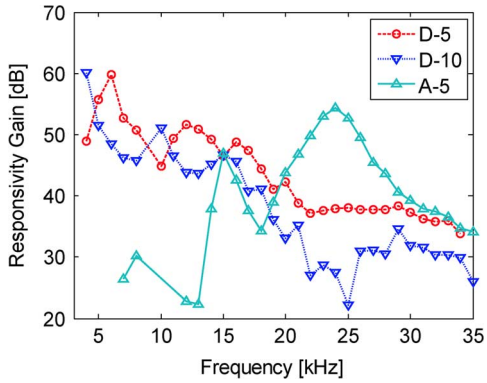

Fig. 9. Experimental RG spectra of sensors D-5, D-10, and A-5.

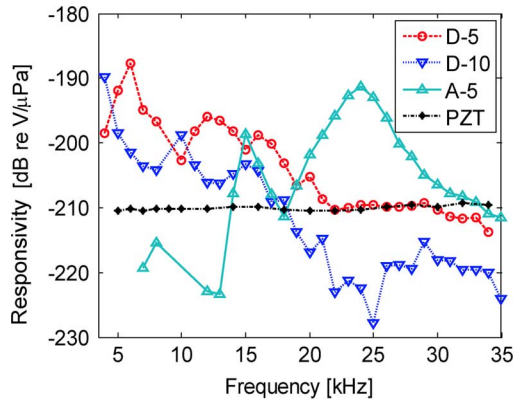

Fig. 10. Experimental responsivity spectra of the three fabricated FBG hydrophones in terms of dB reV/μPa. The responsivity of the PZT reference hydrophone is also shown.

based sensor is significantly shifted toward higher frequencies by comparison with those of the Damival sensors (D-5 and D-10).

For a better understanding of the influence of the coating material on the resonant behavior of FBG hydrophones, the experimental RG spectra of sensors D-5 and A-5 are compared in Fig. 9.

Such comparison confirms the numerically predicted possibility to tune the acoustic resonances of FBG-based hydrophones by exploiting coating materials with different characteristics. In particular, it was found that increasing the elastic modulus decreases the background RG (e.g., the RG of sensor A-5 significantly drops before 15 kHz) and shifts resonances toward higher frequencies (from $\sim$ 6 kHz of the Damival sensor to $\sim$ 24 kHz of the Araldite counterpart).

From the aforementioned results, the possibility to optimize and tailor the acoustic performance of optical hydrophones by means of a judicious selection of the coating material is envisaged [27], [28]. These results are also more significant if one recalls that, based on the theoretical model available in the literature [20], [21], a responsivity increase of FBG-based acoustic sensors could be expected only by decreasing Young's modulus of the coating material, without taking into account the effects, induced by the acousto-mechanical features of the involved materials, on the free vibration modes of the composite structure.

Similarly, by comparing the experimental RG spectra of sensors D-5 and D-10, the effect of the coating diameter may also be inferred. To this aim, the RGs of the two optical hydrophones are superimposed in Fig. 9. It can be observed that, in agreement with the numerical predictions in Section II, the resonances downshifted (from $\sim$6 kHz to 4 kHz) by increasing the cylindrical coating diameter from 5 to 10 mm. Furthermore, the background responsivity (in particular the first minimum between two adjacent resonances) remains quite stable with the diameter. This is also in agreement with the numerical prediction in Section II, where a saturation behavior was observed, consistent with the static prediction [27]–[29].

Finally, it can be noticed that the cutoff frequency of the "low-pass" behavior exhibited by the background responsivity decreases with the diameter. This is also attributable to the previously mentioned acoustic-diffraction effects. We stress also that this result may be predicted by our numerical simulations [34], whereas it could not be account for by using a static model [27]–[29].

C. FBG Hydrophones Performances

In order to compare the spectral behavior of the optical hydrophones with that of the reference PZT, the responsivities of the four devices, calculated as dB re V/μPa [9], are shown in Fig. 10.

It can be seen that the responsivities of the optical devices based on Damival coatings are significantly higher than that of the reference PZT within the range 4–21 kHz, whereas for higher frequencies, they strongly decrease (probably due to the acoustic wave scattering).

On the contrary, the responsivity of the Araldite-based device results is significantly higher than the PZT reference hydrophone for higher frequencies due to the sensor resonance at $\sim$24 kHz, with responsivity ~ -191.3 dB re V/μPa (by comparison with -209 dB re V/μPa for the reference PZT).

From the aforementioned results, and taking into account the noise floor of the setup utilized (currently not optimized), a minimum detectable acoustic signal of about 10 mPa/Hz$^{1/2}$ can be obtained around the resonances of both Damival and Araldite hydrophones.

Although the experimentally demonstrated responsivities are comparable with those of PZT detectors, the achieved limit of detection is higher (worse) than that required for passive acoustic detection, and an improvement of at least two orders of magnitude is necessary for practical implementations.

Nevertheless, on the basis of the results presented, the coated FBGs could efficiently work in realistic (though niche) applications dealing with active acoustic detection where the resonant behavior could be efficiently adopted in combination with suitable synchronous demodulation schemes.

Moreover, our results demonstrated a significant improvement up to three orders of magnitude with respect to the state of the art of passive FBG sensors for underwater acoustic sensing. Furthermore, the present investigation provides a clear understanding of the physical mechanism at the basis of the observed resonant behavior, setting the stage to suitable performance tailoring for specific applications.

Finally, we believe that the idea of exploiting ring-shaped coatings to enhance the responsivity within and far from resonances could be usefully extended also to other fiber sensors configurations (such as DFB laser).

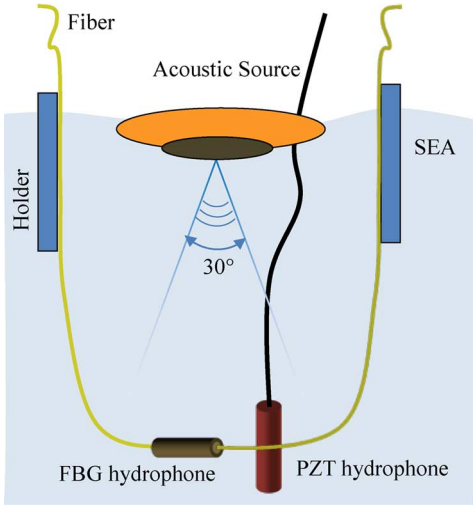

Fig. 11. Schematic of the wet part of the experimental setup utilized in the offshore testing.

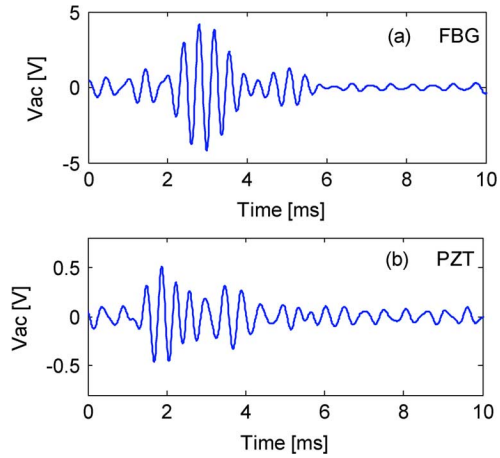

Fig. 12. Typical time responses in terms of acquired voltage changes of (a) FBG sensor D-5 and (b) PZT reference hydrophone.

V. Offshore Testing

We finally move on to illustrate some preliminary results from an offshore testing, which was aimed at assessing the capability of ring-shaped coated FBG hydrophones to be exploited in open environment for practical applications.

The demonstration was held in the Bacoli (Naples) bay off the south-western cost of Italy, by using a suitably equipped boat. During the demonstration, the advantages of using a fiber hydrophones over bulkier PZT counterparts became clearly evident.

The wet part of the experimental setup (i.e., the one immersed or in contact with the sea) is schematically depicted in Fig. 11, and consists of an acoustic source (Uniboom EG&G), a coated FBG sensor (in this case, sensor D-5), and a PZT hydrophone (Type 8100, from Bluel & Kjaer) as reference device.

The acoustic source emits a wideband acoustic pressure signal within the frequency range 0.4–8 kHz with an emission angle of $\sim 30^\circ$. It was properly arranged at the water level by means of a small inflatable boat tied to the main boat.

The FBG hydrophone was immersed in the sea by fixing the lead-in and lead-out fibers to two buoyant holders, kept separate from the source. This ensures that the sound pressure impinges on the FBG orthogonally to the fiber axis, similarly to the previous experiments.

Finally, the PZT hydrophone, exhibiting a nominal responsivity of -205 dB reV/μPa in the investigated acoustic frequency range, was used as a reference sensor, and located close to the FBG. The FBG and PZT devices were positioned at a distance of ~ 2 m from the source, thereby ensuring their complete inclusion within the acoustic irradiation cone.

The dry part of the experimental setup (i.e., that outside the water) consists of the acoustic source driver and the interrogation systems for both the optical and electrical hydrophones. The optical sensor was interrogated by means of the same interrogation systems used in the in-tank characterization. However, in the offshore testing, a different electronic conditioning circuit was exploited (taking into account the different frequency range of the emitted acoustic signal), exhibiting a gain of ~ 33 dB over the frequency range 1–8 kHz. The same considerations hold for the electrical reference device, whose output signal was processed by a dedicated circuit.

Fig. 12(a) and (b) shows the typical time response (in volt) of sensor D-5 and the PZT reference hydrophone to an impinging acoustic pressure pulse of few millisecond duration.

It can be clearly seen that the responses of both devices are very similar from a qualitative viewpoint, while the difference in the amplitudes is mainly due to the different read-out systems exploited in the two cases. These preliminary results clearly confirm the great potential of optical hydrophone based on coated FBG, and the perspectives for their future exploitation in practical acoustic monitoring applications.

Moreover, we point out that further work is currently in progress aimed at fabricating and testing FBG hydrophone arrays arranged in a linear configuration to be immersed in water without using the buoyant holders, thereby resulting in a simpler solution better suited to practical offshore measurements.

VI. Conclusion

In this paper, we have reported the results of a performance analysis of FBG hydrophones for underwater sound pressure detection, carried out within the frequency range 4–35 kHz. The optical hydrophones investigated consist of FBG sensors coated with cylindrically shaped coatings with different diameters and materials.

Our experimental results confirmed the expected resonant behavior of such devices (recently demonstrated via numerical simulations but not yet validated experimentally), and are in quite good agreement with the numerical predictions. Our results revealed the possibility to properly tailor the FBG hydrophones responsivity via suitable choice of the coating material and geometry, thereby opening up new venues for the optimization and tailoring of acoustic performance of optical hydrophones for specific applications.

Optical hydrophones based on coated FBG exhibited an excellent capability to detect acoustic waves in the investigated frequency range, with extremely high responsivities. More specifically, by adopting a simple interrogation system based on edge-triggered narrow-band interrogation, a minimum detectable acoustic signal of about 10 mPa/Hz$^{1/2}$ and good linearity were obtained without using active configurations.

Preliminary results of an offshore testing carried out in the Bacoli bay (Naples, Italy) provided further confirmation of the great potential of the proposed technology for practical acoustic monitoring applications.

ACKNOWLEDGMENT

The authors gratefully acknowledge support from Dr. A. Giordano (Parthenope University of Naples, Naples, Italy) in the preliminary offshore measurements, from the Whitehead Alenia Sistemi Subacquei (WASS, Italy) for making available the instrumented water tank, and from Prof. L. Palmieri (University of Padova, Padova, Italy) for the numerical simulations.

REFERENCES

[1] J. H. Cole, R. L. Johnson, and P. G. Bhuta, "Fiber optic detection of sound," *J. Acoust. Soc. Amer.*, vol. 62, no. 5, pp. 1136–1138, Nov. 1977.

[2] J. A. Bucaro, H. D. Dardy, and E. F. Carome, "Fiber optic hydrophone," *J. Acoust. Soc. Amer.*, vol. 62, no. 5, pp. 1302–1304, Nov. 1977.

[3] J. R. Lee and H. Tsuda, "Sensor application of fibre ultrasonic waveguide," *Meas. Sci. Technol.*, vol. 17, no. 4, pp. 645–652, Apr. 2006.

[4] G. Wild and S. Hinckley, "Acousto-ultrasonic optical fiber sensors: Overview and state-of-the-art," *IEEE Sensors J.*, vol. 8, no. 7, pp. 1184–1192, Jul. 2008.

[5] B. Culshaw, G. J. Thursby, D. Betz, and B. L. Sorazu, "The detection of ultrasound using fiber-optic sensors," *IEEE Sensors J.*, vol. 8, no. 7, pp. 1360–1367, Jul. 2008.

[6] G. Thursby, B. Sorazu, D. Betz, W. Staszewski, and B. Culshaw, "The use of fibre optic sensors for damage detection and location in structural materials," *Appl. Mech. Mater.*, vol. 1–2, pp. 191–196, 2004.

[7] C. Kirkendall and A. Dandridge, "Overview of high performance fibre optic sensing," *J. Phys. D: Appl. Phys.*, vol. 37, no. 18, pp. R197–R216, Sep. 2004.

[8] N. Takahashi, A. Hirose, and S. Takahashi, "Underwater acoustic sensor with fiber Bragg grating," *Opt. Rev.*, vol. 4, no. 6, pp. 691–694, Nov. 1997.

[9] D. C. Betz, G. Thursby, B. Culshaw, and W. Staszewski, "Acousto-ultrasonic sensing using fiber Bragg gratings," *Smart Mater. Struct.*, vol. 12, no. 1, pp. 122–128, Feb. 2003.

[10] D. C. Betz, G. Thursby, B. Culshaw, and W. Staszewski, "Identification of structural damage using multifunctional Bragg grating sensors: I. Theory and implementation," *Smart Mater. Struct.*, vol. 15, no. 5, pp. 1305–1312, Oct. 2006.

[11] H. Tsuda, E. Sato, T. Nakajima, H. Nakamura, T. Arakawa, H. Shiono, M. Minato, H. Kurabayashi, and A. Sato, "Acoustic emission measurement using a strain-insensitive fiber Bragg grating sensor under varying load conditions," *Opt. Lett.*, vol. 34, no. 19, pp. 2942–2944, Oct. 2009.

[12] P. Wierzba and P. Karioja, "Modelling of active fiber Bragg grating underwater acoustic sensor," in *Proc. SPIE*, Nov. 2004, vol. 5576, pp. 348–354.

[13] D. J. Hill and P. J. Nash, "In-water acoustic response of a coated DFB fibre laser sensor," in *Proc. SPIE*, 2000, vol. 4185, pp. 33–36.

[14] S. Foster, A. Tikhomirov, M. Milnes, J. van Velzen, and G. Hardy, "A fibre laser hydrophone," in *Proc. SPIE*, Aug. 2005, vol. 5855, pp. 627–630.

[15] N. Takahashi, K. Yoshimura, S. Takahashi, and K. Imamura, "Development of an optical fiber hydrophone with fiber Bragg grating," *Ultrasonics*, vol. 8, no. 1–8, pp. 581–585, Mar. 2000.

[16] S. Tanaka, H. Yokosuka, and N. Takahashi, "Temperature-stabilized fiber Bragg grating underwater acoustic sensor array using incoherent light," in *Proc. SPIE*, 2005, vol. 5855, pp. 699–702.

[17] S. Tanaka, H. Yokosuka, and N. Takahashi, "Temperature-independent fiber Bragg grating underwater acoustic sensor array using incoherent light," *Acoust. Sci. Technol.*, vol. 27, no. 1, pp. 50–52, 2006.

[18] N. Takahashi, K. Tetsumura, and S. Takahashi, "Multipoint detection of an acoustical wave in water with WDM fiber Bragg grating sensor," in *Proc. SPIE*, Jun. 1999, vol. 3740, pp. 270–273.

[19] H. Yokosuka, S. Tanaka, and N. Takahashi, "Time-division multiplexing operation of temperature-compensated fiber Bragg grating underwater acoustic sensor array with feedback control," *Acoust. Sci. Technol.*, vol. 26, no. 5, pp. 456–458, Sep. 2005.

[20] S. Goodman, A. Tikhomirov, and S. Foster, "Pressure compensated distributed feedback fibre laser hydrophone," in *Proc. SPIE*, May 2008, vol. 7004, pp. 700426-1–700426-4.

[21] W. Zhang, Y. Liu, F. Li, and H. Xiao, "Fiber laser hydrophone based on double diaphragms: Theory and experiment," *J. Lightw. Technol.*, vol. 26, no. 10, pp. 1349–1352, May 2008.

[22] L. Ma, H. Yongming, L. Hong, and H. Zhengliang, "DFB fiber laser hydrophone with flat frequency response and enhanced acoustic pressure sensitivity," *IEEE Photon. Technol. Lett*, vol. 21, no. 17, pp. 1280–1282, Sep. 2009.

[23] S. Goodman, S. Foster, J. van Velzen, and H. Mendis, "Field demonstration of a DFB fibre laser hydrophone seabed array in Jervis Bay, Australia," in *Proc. SPIE*, 2009, vol. 7503, pp. 75034L1–75034L4.

[24] S. Foster, A. Tikhomirov, and J. van Velzen, "Towards a high performance fiber laser hydrophone," *J. Lightw. Technol.*, vol. 29, no. 9, pp. 1335–1342, May 2011.

[25] G. A. Cranch, G. M. H. Flockhart, and C. K. Kirkendall, "Distributed feedback fiber laser strain sensors," *IEEE Sensors J.*, vol. 8, no. 7, pp. 1161–1172, Jul. 2008.

[26] D. J. Hill and G. A. Cranch, "Gain in hydrostatic pressure sensitivity of coated fiber Bragg grating," *Electron. Lett.*, vol. 35, no. 15, pp. 1268–1269, Jul. 1999.

[27] G. B. Hocker, "Fiber optic acoustic sensors with composite structure: An analysis," *Appl. Opt.*, vol. 18, no. 21, pp. 3679–3683, Nov. 1979.

[28] G. B. Hocker, "Fiber-optic acoustic sensors with increased sensitivity by use of composite structures," *Opt. Lett.*, vol. 4, no. 10, pp. 320–321, Oct. 1979.

[29] G. B. Hocker, "Fiber-optic sensing of pressure and temperature," *Appl. Opt.*, vol. 18, no. 9, pp. 1445–1448, May 1979.

[30] Y. Liu, Z. Guo, Y. Zhang, K. S. Chiang, and X. Dong, "Simultaneous pressure and temperature measurement with polymer-coated fiber Bragg grating," *Electron. Lett.*, vol. 36, no. 6, pp. 564–566, Mar. 2000.

[31] A. Cusano, S. D'Addio, A. Cutolo, S. Campopiano, M. Balbi, S. Balzarini, and M. Giordano, "Enhanced acoustic sensitivity in polymeric coated fiber Bragg grating," *Sens. Trans. J.*, vol. 82, no. 8, pp. 1450–1457, Aug. 2007.

[32] S. Campopiano, A. Cutolo, A. Cusano, M. Giordano, G. Parente, G. Lanza, and A. Laudati, "Underwater acoustic sensors based on fiber Bragg gratings," *Sensors*, vol. 9, no. 6, pp. 4446–4454, Jun. 2009.

[33] M. Moccia, M. Pisco, A. Cutolo, V. Galdi, and A. Cusano, "Resonant hydrophones based on coated fiber Bragg gratings—Part I: Numerical analysis," in *Proc. SPIE*, May 2011, vol. 7753, pp. 775384-1–775384-4.

[34] M. Moccia, M. Pisco, A. Cutolo, V. Galdi, P. Bevilacqua, and A. Cusano, "Resonant behavior of coated fiber Bragg gratings as underwater acoustic sensors," *Opt. Exp.*, vol. 19, no. 20, pp. 18842–18860, Sep. 2011.

[35] M. Moccia, M. Consales, A. Iadicicco, M. Pisco, A. Cutolo, and A. Cusano, "Resonant hydrophones based on coated fiber Bragg gratings. Part II: Experimental analysis," in *Proc. SPIE*, May 2011, vol. 7753, pp. 775383-1–775383-4.

[36] Huntsman Advanced Materials [Online]. Available: www.huntsman-service.com/Product_Finder/ui/PSDetailCompositeList.do?pInfoSBUId=9&PCId=1663

[37] [Online]. Available: http://www.efunda.com/materials/polymers/properties/polymer_datasheet.cfm?MajorID=PU&MinorID=1

[38] T. Pritz, "The Poisson's loss factor of solid viscoelastic materials," *J. Sound Vibrat.*, vol. 306, no. 3–5, pp. 790–802, Oct. 2007.

[39] A. Sorathia, "Polyurethane-Epoxy Interpenetrating Polymer Network Acoustic Damping Material," U.S. Patent 5 331 062, July 19, 1994.

[40] F. A. Khayyat and P. Stanley, "The dependence of the mechanical, physical and optical properties of Araldite CT200/HT 907 on temperature over the range -10°C to 70°C," *J. Phys. D: Appl. Phys.*, vol. 11, no. 8, pp. 1237–1247, Jun. 1978.

[41] F. J. P. Chaves, "Application of adhesive bonding in PVC windows" M.Sc Thesis, University of Porto, Porto, Portugal, 2005 [Online]. Available: http://www.scribd.com/doc/37203644/MSc-Thesis

[42] B. Möller Chemie, Technical Data: PUR and Epoxy [Online]. Available: http://www.bm-chemie.de/content/de/download/pub/Elektrogiessharze_12_03_2009.pdf

[43] J. Preisig, "Acoustic propagation considerations for underwater acoustic communications network development," in *Proc. 1st ACM Int. Workshop Underwater Netw.*, Los Angeles, CA, Sep. 25, 2006, pp. 1–5.

Massimo Moccia was born in Benevento, Italy, on February 11, 1982. He received the B.S. and M.S. degrees in telecommunications engineering (*summa cum laude*) from the University of Sannio, Benevento, in January 2005 and May 2007, respectively, where he is currently working toward the Ph.D. degree in information engineering.

His research interests include optoelectronic acoustic sensors based on fiber Bragg gratings.

Mr. Moccia won the "OFS'2011 Student Paper Award" at the 21th International Conference on Optical Fibre Sensors, Ottawa, Canada, in May 2011.

Marco Consales was born in Benevento, Italy, on December 11, 1979. He received the Laurea degree in telecommunications engineering (*summa cum laude*) in January 2004 from the University of Naples Federico II, Italy and the Ph.D. degree in information engineering from the University of Sannio, Benevento, in 2007.

In the same year, he was awarded with the "IEEE-LEOS Best Doctoral Thesis Award in Optoelectronics" from the IEEE-LEOS Italian Chapter. In March 2004, he started his research in the Engineering Department of the University of Sannio, where he was involved in optical fiber sensors for environmental monitoring. In May 2004, he won a fellowship for the XIX Ph.D. course (with tutor Prof. A. Cutolo and Prof. A. Cusano), which was focused on the development of fiber-optic sensors based on nanostructured functional materials. He is currently an Assistant Professor at the University of Sannio. His research activity is focused on the area of advanced optoelectronics and photonics devices for chemical, biological and environmental applications as well as for industrial applications. He is the coauthor of two national patents, 7 invited book chapters, about 30 scientific publications on relevant peer-reviewed international scientific journals, and more than 50 publications on national and international conference proceedings.

Dr. Consales is also in the Editorial board of the Journal of Sensors (Hindawi Publishing Corporation) and acts as a referee for several scientific international journals of the Institute of Physics, Elsevier and IEEE.

Agostino Iadicicco was born in Italy in 1974. He received the degree (*cum laude*) in electronic engineering from the Second University of Naples, Naples, Italy, in 2002, and the Ph.D. degree in information engineering from the University of Sannio, Benevento, Italy, in 2005.

He currently holds a permanent position as Assistant Professor at the Parthenope University of Naples, Naples. His research interests include the area of fiber-optic devices. In particular, he is mainly involved in the design and prototyping of novel devices based on fiber Bragg gratings and long-period gratings in standard and new generation optical fibers for sensors and communications application.

Marco Pisco was born in Naples, Italy, in 1977. He received the degree in information and telecommunication engineering from the University of Naples Federico II, Naples, in 2003, and the Ph.D. degree from the University of Sannio, Benevento, Italy, in joint with the Faculty of Electrical Engineering, University of Zagreb, Zagreb, Croatia, in 2007.

He is currently a Postdoctoral Researcher in the Optoelectronic Division, Department of Engineering, University of Sannio. His research interests include the areas of optoelectronic sensors and photonic bandgap-based devices for sensing and communication applications. He is the author or coauthor of several international publications, including international journals, conferences, and books' chapters and reviewer for the IEEE, the Optical Society of America, and Elsevier journals.

Antonello Cutolo born in Naples, Italy, on November 7, 1955. He received the doctoral degree in electronic engineering from the University of Naples Federico II, Naples, Italy.

After serving the Italian Air Force, he was with the Applied Mathematics and Physics Laboratory, Technical University of Denmark (during 1980–1981). From 1981 to 1983, he was with Adone Storage Ring of Frascati to build a free electron laser (FEL). From 1983 to 1986, he was with the High Energy Physics Laboratory, Stanford, CA, where he was in charge of the broadband optical resonators, diagnostic equipment, and harmonic generator for the infrared FEL. In 1987, he was with Duke University. In 1986, he was a Professor of quantum electronics at the University of Naples, Naples, where he became a Professor of optoelectronics in 1993. He is currently a Full Professor at the University of Sannio, Benevento, Italy. His research interests include fiber-optic sensors, optoelectronic modulators and switching, laser beam diagnostic, and nonlinear optical devices.

Vincenzo Galdi (M'98–SM'04) was born in Salerno, Italy, on July 28, 1970. He received the Laurea degree (*summa cum laude*) in electrical engineering and the Ph.D. degree in applied electromagnetics from the University of Salerno, Salerno, in 1995 and 1999, respectively.

From April to December 1997, he held a visiting position in the Radio Frequency Division, European Space Research and Technology Centre, Noordwijk, The Netherlands. From September 1999 to August 2002, he was a Postdoctoral Research Associate in the Department of Electrical and Computer Engineering, Boston University, Boston, MA, and at the Center for Subsurface Sensing and Imaging Systems, Boston. He is currently in the Department of Engineering, University of Sannio, Benevento, Italy, where he has been an Associate Professor of electromagnetics since November 2002. He has served as an Associate Chair for Undergraduate Studies in Telecommunication Engineering (during 2005–2010), and has been serving as the Delegate reporting to the Dean of Engineering regarding teaching matters since 2007. He is an Associate of the Italian National Institute of Nuclear Physics and of the SPIN Institute, National Research Council. During July–August 2006, within the framework of the Laser Interferometer Gravitational-wave Observatory (LIGO) experiment, he held a visiting position at the Massachusetts Institute of Technology, Cambridge, MA, and at the California Institute of Technology, Pasadena. He is the author or coauthor of nearly 200 papers published in peer-reviewed international journals, books, and conference proceedings, and is a regular reviewer for several journals, conferences, and funding agencies. His research interests include analytical and numerical techniques for wave propagation in complex environments, metamaterials, electromagnetic chaos, inverse scattering, and gravitational interferometry.

Dr. Galdi is the recipient of the 2001 International Union of Radio Science "Young Scientist Award." He is a member of Sigma Xi, of the LIGO Scientific Collaboration, and of the Italian Electromagnetic Society.

Andrea Cusano was born in Caserta, Italy, on May 31, 1971. He received the Master's degree (*cum laude*) in electronic engineering from the University of Naples "Federico II," Naples, Italy, on November 27, 1998, where he also received the Ph.D. degree in information engineering (with tutor Prof. A. Cutolo).

He is currently an Associate Professor at the University of Sannio, Benevento, Italy. Since 1999, his research activity has been focused in the field of optoelectronic devices for sensing and telecommunication applications. He was the cofounder of the spin-off company "OptoSmart S.r.l." in 2005 and of the spin-off company "MDTech" in 2007. He has contributed to more than 100 papers on prestigious international journals and more than 150 communications in well-known international conferences worldwide. He has four international patents currently in charge of prestigious industrial companies (Ansaldo STS, Alenia WASS, Optosmart, and MdTEch) and more than ten national patents. He is also the referee of several scientific international journals. He was a principal investigator and scientific responsible of several national and international research projects. He is the coauthor of more than ten chapters published in international books and invited papers in prestigious scientific international journals. He is the coeditor of three scientific international books. He is also a consultant for big companies of the Finmeccanica group such as Ansaldo STS and Alenia WASS. He has also collaborations with the European Organization for Nuclear Research, Geneva, Switzerland, where he is involved in the development of innovative sensors for high-energy physics applications.

Dr. Cusano is an Associate Editor of the *Sensors and Transducers Journal*, the *Journal of Sensors* (Hindawi), The *Open Optics Journal* (Bentham), The *Open Environmental & Biological Monitoring Journal* (Bentham), and the *International Journal on Smart Sensing and Intelligent Systems*. He is a member of the technical committee of several international conferences such as the IEEE Sensors, the International Conference on Space Technology, the European Workshop on Structural Health Monitoring, and the European Workshop on Optical Fibre Sensors. He is the coeditor of two Special Issues: Special Issue on Optical Fiber Sensors, IEEE Sensors 2008, and Special Issue on "Fiber Optic Chemical and Biochemical Sensors: Perspectives and Challenges approaching the Nano-Era," Current Analytical Chemistry, Bentham, 2008.